Optical Evidence for Symmetry Changes above the Néel Temperature of $KCuF_3$

J. Deisenhofer,[1] I. Leonov,[2] M. V. Eremin,[3] Ch. Kant,[4] P. Ghigna,[5] F. Mayr,[4] V. V. Iglamov,[3] V. I. Anisimov,[6] and D. van der Marel[1]

[1]*Département de Physique de la Matière Condensée, Université de Genève, CH-1211 Genève 4, Switzerland*
[2]*Abdus Salam International Centre for Theoretical Physics, Trieste 34014, Italy*
[3]*Kazan State University, 420008 Kazan, Russia*
[4]*EP 5, EKM, Institute for Physics, Augsburg University, D-86135 Augsburg, Germany*
[5]*Dipartimento di Chimica Fisica "M. Rolla," Università di Pavia, I-27100 Pavia, Italy*
[6]*Institute of Metal Physics, 620219 Yekaterinburg GSP-170, Russia*

(Received 13 April 2007; revised manuscript received 5 August 2008; published 10 October 2008)

We report on optical measurements of the 1D Heisenberg antiferromagnet $KCuF_3$. The crystal-field excitations of the Cu^{2+} ions have been observed and their temperature dependence can be understood in terms of magnetic and exchange-induced dipole mechanisms and vibronic interactions. Above T_N we observe a new temperature scale T_S characterized by the emergence of narrow absorption features that correlate with changes of the orbital ordering as observed by Paolasini *et al.* [Phys. Rev. Lett. **88**, 106403 (2002)]. The appearance of these optical transitions provides evidence for a symmetry change above the Néel temperature that affects the orbital ordering and paves the way for the antiferromagnetic ordering.

DOI: 10.1103/PhysRevLett.101.157406 PACS numbers: 78.20.Ls, 71.70.Ej, 75.40.−s, 78.40.−q

The charge-transfer insulator $KCuF_3$ is a prototype material for a cooperative Jahn-Teller (JT) effect, orbital ordering (OO), and low-dimensional magnetism [1]. $KCuF_3$ stands in line with $LaMnO_3$, the parent compound of the colossal magnetoresistance manganites, as role models for orbitally ordered compounds, where collective orbital modes may occur in the excitation spectrum [2,3]. Moreover, $KCuF_3$ is one of the rare examples of an ideal one-dimensional (1D) antiferromagnetic (AFM) Heisenberg chain. This is related to the particular OO in $KCuF_3$, in which a single hole alternately occupies $3d_{x^2-z^2}$ and $3d_{y^2-z^2}$ orbital states of the Cu^{2+} ions with a $3d^9$ electronic configuration [4]. The cooperative JT distortion is characterized by CuF_6 octahedra elongated along the a and b axis and arranged in an antiferrodistortive pattern in the ab plane. A crossover from a 1D to a 3D behavior occurs at the Néel temperature $T_N = 39$ K resulting in a long-range (A-type) AFM ordering, but the fingerprint of a 1D spin chain, the spinon excitation continuum, is still observable below T_N and persists up to about 200 K [5]. Together with a strong suppression of the ordered moment found below T_N, this establishes the impact of quantum fluctuations on the magnetism of $KCuF_3$ [6].

To date, even the room temperature (RT) crystal structure of $KCuF_3$ seems not to be determined unambiguously. The original assignment of tetragonal symmetry [7] was challenged by the claim of an orthorhombic structure [8]. Although such a distortion seems to allow for a better understanding of Raman [9] and electron paramagnetic resonance properties [10], discrepancies remain when trying to reconcile the observation of AFM resonances within the proposed symmetries [11]. Paolasini and co-workers reported an x-ray resonant scattering (XRS) study of the OO-superlattice reflection in $KCuF_3$ and found a considerable increase of its intensity above T_N, indicating changes of the lattice degrees of freedom prior to magnetic ordering [12,13].

Here we report optical spectra of the crystal-field (CF) excitations in $KCuF_3$ in the near infrared range. The observed energy splittings are compared to theoretical estimates using crystal-field theory (CFT) and to a direct calculation in the framework of local density approximation (LDA) [14]. Furthermore, we discovered the appearance of a very sharp fine structure related to the d-d absorption bands below $T_S = 50$ K, which is interpreted as a new temperature scale above T_N, where a dynamic distortion of the environment of the Cu^{2+} ions becomes static.

The single crystals (see Ref. [12] for details on crystal growth) were oriented by Laue diffraction and cut along the (110) plane. Polarization-dependent transmission measurements were performed using a Bruker IFS 66v/S Fourier-transform spectrometer with an Oxford ^{4}He cryostat in the frequency range between 5000–16 000 cm^{-1} and for temperatures from 4–300 K. The absorption coefficient α was obtained using the standard relation for a semitransparent layer [15] and $\sigma_1 = \alpha n c \epsilon_0$ was obtained by estimating the refractive index n from $\epsilon_1 \approx 2.2$ given by ellipsometry data at RT. This value is in good agreement with $\epsilon_1 \approx 2.3$ obtained theoretically [16].

In Fig. 1(a) we show the absorption coefficient α for light polarized parallel ($\mathbf{E} \parallel c$) and perpendicular ($\mathbf{E} \perp c$) to the antiferromagnetically coupled c axis at 8 K. For both orientations one can identify four broad excitation bands which are indicated by arrows and called A_1–A_4 in the following. The onset and maximum energies of these bands are given in Table I. One can recognize rather symmetric line shapes for A_1 and A_4, while A_2 exhibits a very asym-

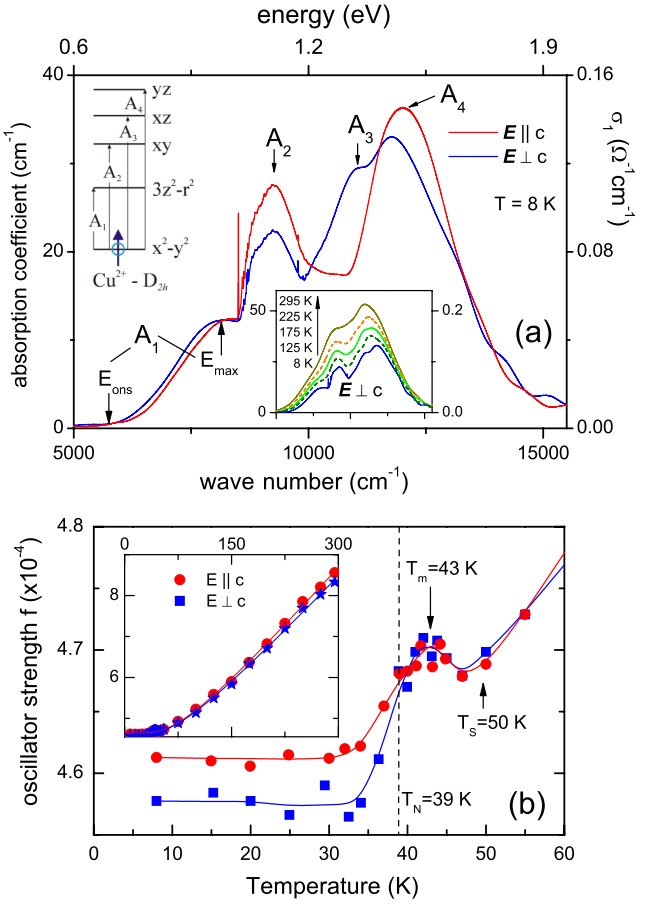

FIG. 1 (color online). (a) Absorption spectra for $E \parallel c$ and $E \perp c$ at 8 K. Arrows indicate the four absorption bands A_1–A_4 related to the CF splitting for Cu^{2+} in D_{2h} *symmetry*. For A_1 the onset energy E_{ons} and the maximum at E_{max} are indicated. Inset: Evolution of absorption spectra with temperature for $E \perp c$. (b) Anomalies of the oscillator strength f above T_N. Lines are guides to the eye. Inset: Full temperature dependence of f. Solid lines are fits described in the text.

metric line shape with a steep absorption edge at the low-energy side. Since A_3 is visible mainly as a shoulder in the spectrum, its line shape is not evident. Moreover, a sharp spikelike feature can be seen at the onset of the A_2 band [see Fig. 2(a) for an enlarged scale), which will be discussed in detail below.

TABLE I. Comparison of E_{ons} and E_{max} for the energies of the onsets and the maxima of bands A_1–A_4 with theoretical estimates E_{CFT}, E_{LDA}, and E_{LDA+U} obtained as described in the text. The energies are given in eV.

	E_{ons}	E_{CFT}	E_{max}	E_{LDA}	E_{LDA+U}
yz	1.34	1.34	1.46	1.62	1.50
xz	1.21	1.26	1.37	1.37	1.41
xy	1.05	1.06	1.15	1.28	1.31
$3z^2 - r^2$	0.71	0.69	1.02	0.94	1.03
$x^2 - y^2$	0	0	0	0	0

Comparing the two spectra in Fig. 1(a) one finds that the intensities of A_2 and A_4 are enhanced for $\mathbf{E} \parallel c$, while A_3 seems to be much more intense for $\mathbf{E} \perp c$. The temperature behavior of the absorption bands is illustrated in the inset of Fig. 1(a) for $\mathbf{E} \perp c$. The bands broaden and gain intensity with increasing temperature. The nature of these absorption bands can be understood in terms of local d-d CF excitations of the Cu^{2+} ions in a distorted octahedral environment [17]. Usually, electric dipole transitions between d levels are parity-forbidden, but they can become allowed as a consequence of a perturbation of the CF potential by phonons. A fingerprint of such *vibronically* allowed transitions is the temperature dependence of their oscillator strength f given by

$$\int_{\omega_1}^{\omega_2} \sigma_1(\omega) d\omega = \frac{\pi}{2} \frac{e^2 N}{m} f, \qquad (1)$$

where N is the number of absorption centers per unit

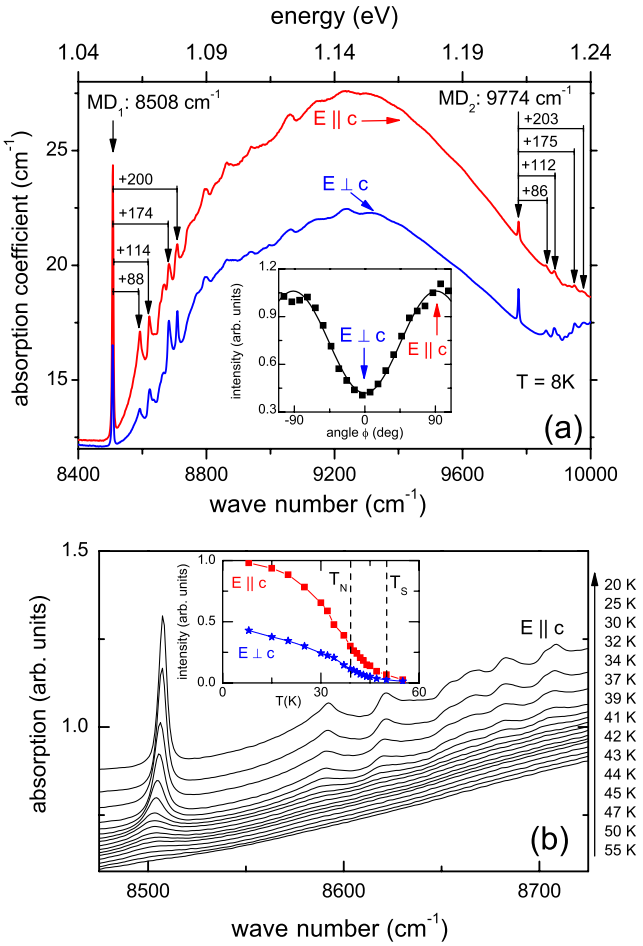

FIG. 2 (color online). (a) Fine structures related to A_2 and A_3 for $E \parallel c$ and $E \perp c$ at 8 K. Frequency shifts with respect to MD_1 and MD_2 are indicated in cm^{-1}. Inset: Polarization dependence of the intensity of MD_1 and a fit $\propto \sin^2\phi$. (b) Emerging of the fine structure peaks below $T_S = 50$ K for $E \parallel c$. Inset: Temperature dependence of the intensity of MD_1 for both orientations. Lines are guides to the eyes.

volume [18]. Assuming that only a single vibrational mode with frequency ω_{vib} contributes to the intensity of the absorption, one expects $f = f_{\mathrm{vib}} \coth(\hbar\omega_{\mathrm{vib}}/2k_BT)$ [18,19]. By adding a temperature independent term f_{mag} one usually accounts for the contribution of magnetic dipole (MD) transitions. The order of magnitude of 10^{-3}–10^{-4} is in agreement with theoretical expectations [18].

We show as an inset in Fig. 1(b) the temperature dependence of f obtained by integration between $\omega_1 = 5000\ \mathrm{cm}^{-1}$ and $\omega_2 = 16\,000\ \mathrm{cm}^{-1}$ for both orientations. Fitted over the whole temperature range from 8–295 K, f appears to be well described (solid lines) by this approach with $\omega_{\mathrm{vib}} = 148, 144\,\mathrm{cm}^{-1}$, $f_{\mathrm{vib}} = 2.1\times10^{-4}, 1.9\times10^{-4}$, and $f_{\mathrm{mag}} = 2.5\times10^{-4}, 2.7\times10^{-4}$ for $\mathbf{E} \parallel c$ and $\mathbf{E} \perp c$, respectively. When zooming in to the low-temperature regime in the vicinity of T_N as shown in Fig. 1(b), one can clearly see deviations from this behavior starting at below a temperature $T_S \approx 50$ K. An additional contribution to f leads to a maximum at around 43 K and a subsequent decrease upon AFM ordering at 39 K towards a constant low-temperature value. Note that the increase below 50 K is directly related to the appearance of the sharp-absorption features at the broad bands A_2 and A_3 [see Fig. 2(a)].

Considering the space group $D_{4h}^{18} - I4/mcm$ [7] and the local D_{2h} symmetry at the Cu^{2+} site, a complete splitting of the CF levels is expected [see Fig. 1(a)]. We compare the experimental splittings to theoretical estimates via two different approaches in Table I. The onset energies E_{ons} of A_1–A_4 correspond to the purely electronic splittings and are estimated by E_{CFT} obtained using the exchange charge model in CFT [20,21]. The calculation describes the experimental splittings nicely and further parameters like anisotropic g values and the nuclear quadrupole resonance properties were derived, in good agreement with experimental data [10,22].

In the second approach, the electronic structure of $KCuF_3$ was calculated self-consistently using LDA($+U$). According to previous LDA calculations [23,24], the Coulomb and exchange interaction parameters U and J were taken to be 8.0 and 0.9 eV, respectively. Following Streltsov *et al.* [14], we additionally estimate $E_{\mathrm{LDA}+U}$ as the difference between the ground state energy and an energy of an excited state in which the hole is artificially put on one of the higher levels by applying constrained LDA + U calculations. This constrained method takes into account the relaxation of the electronic system, whereas the lattice remains frozen obeying the Franck-Condon principle. Hence, the resulting CF splittings have to be compared with E_{max} of the absorption bands in Table I. Both calculations describe the experimental findings, but including electronic relaxation gives an overall better agreement between theory and experiment.

Having described the origin of the broadband spectra on a quantitative level, we now concentrate on the observation of two sets of sharp-absorption features highlighted in Fig. 2(a), one indicating the onset of A_2 at 8508 cm^{-1} followed by a whole sideband of excitations, and a second set starting at 9775 cm^{-1} at the anticipated onset of A_3. Both sets are visible for $\mathbf{E} \parallel c$ and $\mathbf{E} \perp c$. As an inset of Fig. 2(a) we show the polarization dependence of the intensity of the peak at 8508 cm^{-1} following a $\sin^2\phi$ dependence, with ϕ being the angle between the polarization and the crystal axes. While the latter peak is more intense for $\mathbf{E} \parallel c$, the peak at 9775 cm^{-1} is more intense for $\mathbf{E} \perp c$. Note that H_z in the local coordinate system corresponds to $\mathbf{B} \perp c$ or $\mathbf{E} \parallel c$ and H_y corresponds to $\mathbf{B} \parallel c$ or $\mathbf{E} \perp c$, with $\mathbf{B} = \mu(T)\mathbf{H}$, where $\mu(T)$ is the permeability which is usually assumed to be one in optical experiments, but can increase significantly upon magnetic ordering. The observed intensity maxima comply with the selection rules for MD transitions.

Concerning the side bands of both MD transitions, we want to emphasize that the strongest features appear at a distance of 88(86), 114(112), 174(175), and 200(203) cm^{-1} from the $\mathrm{MD}_1(\mathrm{MD}_2)$ transitions [see Fig. 2(a)]. To understand the origin of the whole entity of MD transitions and their sidebands, we have to consider their temperature dependence, which is displayed in Fig. 2(b) for $\mathbf{E} \parallel c$. The fine structure emerges only below a temperature $T_S = 50$ K, the temperature where the overall oscillator strength starts to deviate from a purely vibrational behavior with a constant contribution from MD transitions [Fig. 1(a)]. The integrated intensity of the MD transition at 8508 cm^{-1} as a function of temperature is shown as an inset in Fig. 2(b) for both polarizations without any anomaly visible at $T_N = 39$ K.

It was shown that magnons can become optically active via an exchange-induced dipole mechanism [25,26], with the optical excitation energy corresponding to the magnon energy at the Brillouin zone boundary. In $KCuF_3$, neutron scattering investigations reported zone boundary energies of magnon excitations at 88.7, 117, and 221 cm^{-1} [6,27]. The first two magnon energies correspond very nicely with the first and second sideband peaks, the third sideband peak is in agreement with a two-magnon process involving the 88.7 cm^{-1} magnon, the fourth would correspond to two-magnon process where both the 88.7 and the 117 cm^{-1} magnon participate. For the 221 cm^{-1} magnon we cannot resolve any sideband in absorption. In this scenario the temperature dependence of the MD transitions and the magnon sidebands below T_S is attributed to the increase of $\mu(T)$ in the vicinity of AFM ordering and can gain additional intensity due to the local spin-spin expectation value $\langle \mathbf{S}_i(\mathbf{S}_{i-1} + \mathbf{S}_{i+1})\rangle$ which contributes to the exchange-induced dipole moment $\sum_j \mathbf{\Pi}_{ij}(\mathbf{S}_i\mathbf{S}_j)$ for the Cu ion at site i. For $\mathbf{E} \parallel c$ the spin-spin correlations in the ab plane are important, for $\mathbf{E} \perp c$ the contributing correlations are the ones along the c axis [26].

Here we would like to point out that an anomalous behavior in birefringence [28] and neutron scattering studies [29] has been reported at around $T_m = 43$ K, exactly the temperature where f exhibits a maximum [Fig. 1(b)].

At the same temperature a significant change of the OO-superlattice reflection at the Cu K edge has been reported by an XRS study [12,13]. Since XRS at the K edge probes the JT distortion induced by the OO [30], the anomaly certainly involves a change in the lattice degrees of freedom. On account of LDA + U calculations it has previously been suggested that the anomalous XRS data might indicate a structural transition [24].

In the literature we find two hints concerning a symmetry lowering in $KCuF_3$: an x-ray diffraction study at RT claiming the presence of an orthorhombic distortion due to a shift of the apical F^- ions connecting the CuF_6 octahedra along the c axis [8] and a Raman study of the phonon modes at 10 K, observing the splitting of two E_g Raman modes [9]. To get a more consistent picture of what happens at $T_S = 50$ K, the temperature dependence of the split Raman modes was investigated and the modes were found to soften strongly with decreasing temperature and split only below $T_S = 50$ K [31]. The occurrence of this splitting $T_S = 50$ K is a clear sign for a reduced (static) lattice symmetry. Moreover, a recent approach allows one to describe the electron paramagnetic resonance properties by assuming that the displacement of the apical F^- ions away from the c axis is dynamic in nature, but becomes static at $T \approx T_N$ [32]. The phonon modes contributing to the oscillation of the F^- ions should soften with decreasing temperature as the displacement of the F ions freezes in and becomes static at $T_S = 50$ K, in agreement with the Raman data. This static distortion manifests itself in an increase of intensity of the MD transitions in optics, a splitting of Raman-active phonons, and the increase in intensity of the orbital-ordering superstructure reflection in XRS (lattice fluctuations produce orbital fluctuations which might reduce the XRS intensity above 43 K). The freezing-in of the distortion leads to an additional magnetic anisotropy via a Dzyaloshinsky-Moriya interaction, which favors the alignment of the spins and allows for the AFM transition to take place at $T_N = 39$ K. Next-nearest-neighbor spin correlations develop already below T_S leading to the observation of optically active magnons via the exchange-induced dipole mechanism.

To summarize, we observed broad phonon-assisted CF excitations of the Cu^{2+} ions with a pronounced fine structure below $T_S = 50$ K. These sharp-absorption peaks are identified as magnetic dipole transitions and optically active magnons gaining intensity due to an exchange-induced dipole moment. We argue that at $T_S = 50$ K a dynamic displacement of F^- ions becomes static and leads to symmetry change of the lattice. Given the fact that, e.g., manganites reportedly exhibit changes of the OO-superlattice reflection as measured by XRS in the vicinity of T_N [33] and softening of Raman-active phonon modes [34], too, one may speculate that the phenomena described in this Letter could be present in many AFM transition metal compounds.

It is a pleasure to thank N. P. Armitage, F. Banfi, N. Binggeli, M. Grüninger, A. B. Kuzmenko, C. Mazzoli, A. Loidl, and D. Zakharov for fruitful discussions. We acknowledge partial support by the BMBF via Contract No. VDI/EKM 13N6917, by the DFG via SFB 484, and by the Swiss NSF through NCCR MaNEP.

[1] S. Kadota *et al.*, J. Phys. Soc. Jpn. **23**, 751 (1967).
[2] E. Saitoh *et al.*, Nature (London) **410**, 180 (2001).
[3] R. Ruckamp *et al.*, New J. Phys. **7**, 144 (2005).
[4] K. I. Kugel and D. I. Khomskii, Sov. Phys. Usp. **25**, 231 (1982).
[5] B. Lake *et al.*, Nature Mater. **4**, 329 (2005).
[6] B. Lake *et al.*, Phys. Rev. Lett. **85**, 832 (2000).
[7] A. Okazaki and Y. Suemune, J. Phys. Soc. Jpn. **16**, 176 (1961).
[8] M. Hidaka *et al.*, J. Phys. Soc. Jpn. **67**, 2488 (1998).
[9] T. Ueda *et al.*, Solid State Commun. **80**, 801 (1991).
[10] I. Yamada *et al.*, J. Phys. Condens. Matter **1**, 3397 (1989).
[11] L. Li *et al.*, J. Phys. Condens. Matter **17**, 2749 (2005).
[12] L. Paolasini *et al.*, Phys. Rev. Lett. **88**, 106403 (2002).
[13] R. Caciuffo *et al.*, Phys. Rev. B **65**, 174425 (2002).
[14] S. V. Streltsov *et al.*, Phys. Rev. B **71**, 245114 (2005).
[15] M. Dressel and G. Grüner, *Electrodynamics of Solids* (Cambridge University Press, Cambridge, England, 2002).
[16] A. E. Nikiforov and S. Yu. Shashkin, Phys. Solid State **38**, 1880 (1996).
[17] The local z direction is along the longest Cu-F bond resulting in a $x^2 - y^2$-orbital ground state.
[18] S. Sugano *et al.*, *Multiplets of Transition Metal Ions in Crystals* (Academic, London, 1970).
[19] M. A. Hitchman and P. J. Cassidy, Inorg. Chem. **18**, 1745 (1979).
[20] M. V. Eremin *et al.*, Phys. Status Solidi B **79**, 775 (1977).
[21] B. Z. Malkin, *Spectroscopy of Solids Containing Rare-Earth Ions*, edited by A. H. Kaplyanskii and R. M. Macfarlane (Elsevier, New York, 1987).
[22] C. Mazzoli *et al.*, J. Magn. Magn. Mater. **242–245**, 935 (2002); **272–276**, 106 (2004).
[23] A. I. Liechtenstein *et al.*, Phys. Rev. B **52**, R5467 (1995).
[24] N. Binggeli and M. Altarelli, Phys. Rev. B **70**, 085117 (2004).
[25] R. L. Greene *et al.*, Phys. Rev. Lett. **15**, 656 (1965).
[26] Y. Tanabe and K. Gondaira, J. Phys. Soc. Jpn. **22**, 573 (1967).
[27] S. K. Satija *et al.*, Phys. Rev. B **21**, 2001 (1980).
[28] K. Iio *et al.*, J. Phys. Soc. Jpn. **44**, 1393 (1978).
[29] D. A. Tennant *et al.*, Phys. Rev. B **52**, 13 381 (1995).
[30] P. Benedetti *et al.*, Phys. Rev. B **63**, 060408 (2001).
[31] V. Gnezdilov *et al.* (unpublished).
[32] M. V. Eremin *et al.*, Phys. Rev. Lett. **101**, 147601 (2008).
[33] Y. Murakami *et al.*, Phys. Rev. Lett. **80**, 1932 (1998);**81**, 582 (1998).
[34] K.-Y. Choi *et al.*, Phys. Rev. B **77**, 064415 (2008).